2014-05

Flexible Transparent Conductive Heater Using Multiwalled Carbon Nanotube Sheet

UTD AUTHOR(S): Daewoong Jung, Maeum Han and Gil Sik Lee

JVSTB Journal of Vacuum Science & Technology B

Flexible transparent conductive heater using multiwalled carbon nanotube sheet

Daewoong Jung, Maeum Han, and Gil S. Lee

Citation: Journal of Vacuum Science & Technology B **32**, 04E105 (2014); doi: 10.1116/1.4876127
View online: http://dx.doi.org/10.1116/1.4876127
View Table of Contents: http://scitation.aip.org/content/avs/journal/jvstb/32/4?ver=pdfcov
Published by the AVS: Science & Technology of Materials, Interfaces, and Processing

Flexible transparent conductive heater using multiwalled carbon nanotube sheet

Daewoong Jung, Maeum Han, and Gil S. Lee[a)]
Department of Electrical Engineering, University of Texas at Dallas, 800 West Campbell Road, Richardson, Texas 75080-3021

(Received 18 February 2014; accepted 30 April 2014; published 9 May 2014)

This paper reports highly flexible, transparent, conducting heaters based on multiwalled carbon nanotube (MWCNT) sheets. The MWCNT sheets were spun directly from a well-aligned MWCNT forest. The fabrication of the MWCNT sheet heater was quite simple and suitable for mass production, requiring only a one-step transferring process, in which the MWCNT sheet is drawn onto the target substrates. This study examined the parameters that affect the heat generation of the MWCNT sheet-based heater; input power, surface area, and thermal conductivity of the substrate. In particular, more effort was focused on how to increase the surface area and contact points between the individual MWCNTs; simple acid treatment and added metal nanoparticles increased the heat performance of the heater dramatically. Moreover, the heaters exhibited durability and flexibility against many bending cycles. Therefore, the MWCNT sheet-based heater can be used for versatile applications requiring transparency, conduction, and flexibility. © *2014 American Vacuum Society*. [http://dx.doi.org/10.1116/1.4876127]

I. INTRODUCTION

Since their discovery in 1991,[1] carbon nanotubes (CNT) have attracted considerable attention over the last two decades owing to their unique structural, mechanical and electrical properties.[2–7] Recently, there has been increasing interest in the use of carbon nanotube-based flexible transparent conducting films (TCFs) for applications in displays and still image recorders.[8,9] The importance of TCFs is further highlighted by their potential extended applications to device systems, such as touch panel screens, smart windows, and sensors, in which TCFs are used as transparent electrodes.[10,11] In particular, TCFs are used as transparent heaters for window defrosters, temperature-controlled liquid crystal displays, and medical equipment, as well as for ensuring the stable operation of electronic devices under harsh environmental conditions.[12–14] Moreover, a considerable number of studies have been investigated for manufacturing proper heating elements due to the issues of power consumption and environmental protection. Typical TCF-heater currently in use is based on indium tin oxide (ITO), which satisfies all the TCF requirements.[15,16] However, its price has doubled over the last ten years due to its limited supply. The most common method for ITO deposition is vacuum sputtering. The fabrication process is both expensive and time consuming, and there are problems with polymer substrates, such as polycarbonate, which tends to degas under vacuum. Furthermore, an ITO film is fragile, which means that it is damaged easily when subjected to mechanical bending deformation.[17,18] This is a serious issue in both the manufacturing yield and lifetime for flexible devices. In addition, chemical reactions occur on the ITO surface when exposed to corrosive or organic materials, resulting in interface intolerance.[15,17–19] This has prompted a search for suitable ITO alternatives, such as CNT, metal nanowire, and graphene.[20–23]

CNT-based film heaters were first proposed by Yoon *et al.*[24] to overcome the limitations of ITO film heaters. His group reported a rapid thermal response of single-walled carbon nanotube (SWCNT) films prepared using a vacuum filtering method. They proposed the use of these SWCNT heaters as vehicle defrosters as a potential application. Kim *et al.*[25] investigated the thermal behavior of transparent film heaters made from SWCNT as well, but a spray coating method was selected for fabricating the heater. They studied temperature dependence of the electrical resistance for the heater in various gas environments. Kang *et al.*[26] also fabricated a SWCNT film heater with an optical transparency of above 95% in visible rays by using the dip-coating method and also discussed the thickness-dependent thermal resistance.

On the other hand, multiwalled carbon nanotube (MWCNT) sheets/yarns have attracted increasing attention since the discovery that continuous sheets/yarns can be pulled from spin-capable MWCNT forest by the van der Waals force between MWCNTs.[27–29] Our group produced transparent, conducting MWCNT sheets by simply spinning MWCNTs.[30–32] A previous study reported that the MWCNT sheets could be used as a transparent heater on a glass substrate.[33,34] They exhibited stable, reliable, and superior thermal characteristics. However, despite the successful demonstration of the MWCNT sheet heaters, the fundamental heat transfer mechanism is not completely understood due to the complex phenomenon of heat dissipation. Moreover, the measured steady-state temperatures were relatively low compared to others[25,35] and should be tested on polymer substrates for flexible applications, such as curved windows. Therefore, in this study, more effort was made to analyze the heat transfer mechanism and evaluate the improved heating performance of the MWCNT sheet heater. The thermal properties of the heater, such as the high steady-state temperature and fast response time, were

a)Electronic mail: gslee@utdallas.edu

enhanced considerably by adding metal nanoparticles to the sheet, which provided many contact points between the individual MWCNTs. Moreover, a simple acid treatment could reduce their sheet resistance (R_s),[36] which means the effective power (V^2/R) can be increased to generate heat.

II. EXPERIMENT

Spin-capable MWCNTs were grown from iron (Fe) films, which were deposited by electron-beam evaporation on Si substrates with an oxidized layer of 400 nm thickness. The thickness of the thin Fe film varied in the range of 5 nm and was monitored by a quartz crystal sensor fixed inside the e-beam evaporation chamber. MWCNT growth was performed in a quartz and stainless steel cylindrical chemical-vapor deposition (CVD) chamber at atmospheric pressure using flows of C_2H_2, He, and H_2 gases. The substrates were introduced into the CVD chamber and ramped up to a set point temperature of 780 °C at a ramping rate of 50 °C/min while flowing He (5 slm) and H_2 (100 sccm). The growth of CNTs was carried out at the same temperature and pressure by adding acetylene gas (100 sccm) to the flow for 5 min. The flow of C_2H_2 gas was turned off, and the sample was cooled down to below 100 °C with continuous H_2 and He gas flows. The dimension of the heater was $1 \times 1.5\,cm^2$, and copper tape was attached at both ends of the MWCNT-sheets on the substrates in order to be used as electrodes. The resulting MWCNT sheets were immersed in nitric acid (HNO_3) to examine the changes in the electrical, thermal characteristics of the MWCNT sheets. Nickel (Ni) was deposited on the CNT sheet by electrodeposition. Detail process of CNT growth and experimental procedure were described in supplementary data.[37]

III. RESULTS AND DISCUSSION

Figure 1 shows the heat generation and losses that occur in the MWCNT sheet when subjected to input power. The heat is generated by the Joule effect in the sheet according to the following equation:[26,38]

$$\Delta Q = V^2/R \cdot \Delta t, \tag{1}$$

where R is the electrical resistance of the heated area, V is the applied voltage, and t is the time. This heat is dissipated in the surrounding air and substrates (glass or polymer). The thermal losses can be classified into three types: conduction to the substrates, convection to the air, and radiation.[39]

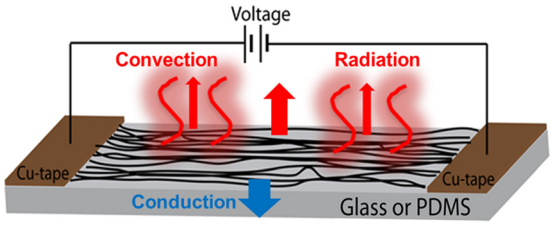

FIG. 1. (Color online) Schematic diagram of the heat losses in a MWCNT sheet-based heater: conduction and convection.

Therefore, the heat generated by the heater is equal to the sum of the heat lost by conduction in the substrates, Q_{cond}, and by convection to the air, Q_{conv} and radiation, Q_{rad}

$$V^2/R \cdot \Delta t = Q_{cond} + Q_{conv} + Q_{rad}. \tag{2}$$

The power (P) can be obtained from Eq. (2) by dividing it by time

$$P = V^2/R = \Delta Q_{cond}/\Delta t + \Delta Q_{conv}/\Delta t + \Delta Q_{rad}/\Delta t, \tag{3}$$

where the power lost by conduction to the substrate is given by

$$\Delta Q_{cond}/\Delta t = \lambda_{cond} \cdot A_{cond} \cdot \Delta T_{cond}/\Delta x. \tag{4}$$

Here, λ_{sub} is the thermal conductivity of the substrate, A_{cond} is the cross-sectional area of the surface of conduction in the substrate, and $\Delta T_{cond}/\Delta x$ is the temperature gradient. To reduce these losses, the substrate should have low thermal conductivity. This will be confirmed shortly.

Second, the power lost by convection to the air can be expressed as

$$\Delta Q_{conv}/\Delta t = h_{conv} \cdot A_{conv} \cdot \Delta T_{conv}, \tag{5}$$

where h_{conv} is a convective heat transfer coefficient, which is a geometrical factor depending on the shape and orientation of the heated surface, A_{conv} is the surface area, and ΔT_{conv} is the temperature difference between the heat source and surrounding environment.

Third, the power lost by radiation is defined as

$$\Delta Q_{rad}/\Delta t = \varepsilon \cdot \sigma \cdot A_{rad} \cdot \Delta T^4, \tag{6}$$

where ε is the emissivity of the material, σ is the Stefan–Boltzmann constant, which is equal to $5.67 \times 10^{-8}\,Wm^{-2}\,K^{-4}$, and A_{rad} is the surface of radiation. Therefore, the total power lost can be obtained by inserting Eqs. (4)–(6) into Eq. (3)

$$V^2/R = \lambda_{cond} \cdot A_{cond} \cdot \Delta T_{cond}/\Delta x + h_{conv} \cdot A_{conv} \cdot \Delta T_{conv} + \varepsilon \cdot \sigma \cdot S_{rad} \cdot \Delta T^4. \tag{7}$$

On the other hand, the losses by radiation can be neglected at the temperature range of interest of the heater due to the very low emissivity of the materials.[26,38] Equation (7) can be simplified further by separating the power lost to the substrate (thermal conduction) and by combining the thermal convection losses in the surrounding media

$$P = V^2/R = \lambda_{cond} \cdot A_{cond} \cdot \Delta T_{cond}/\Delta x + h_{conv} \cdot A_{conv} \cdot \Delta T_{conv}, \tag{8}$$

where h is the experimental value, which is dependent on the environmental parameters.

The transport of thermal energy, from hot to cold regions in a material, is heat (thermal) conduction. Heat conduction

in solid materials is caused by lattice vibrations and free electrons. The heat transfer by free electron is more efficient than the lattice phonon contribution in pure metal, while the lattice vibration is dominant in nonmetallic materials such as polymer or glass due to shortage of free electrons, which results in the propagation of quanta energy called phonons. For steady-state heat conduction, the heat flux is proportional to the temperature gradient along the direction of flow in the material and the thermal conductivity is the proportionality constant.[40]

Therefore, heat generation relies on the input power, thermal conductivity of the substrates, and the surface area of heater. The electro-heating performance of the CNT sheet (Fig. 2) was examined by applying direct voltage power to the sheet under ambient conditions. As shown in Fig. 3(a), the temperature on the surface of the sheet increased monotonically over the input power until a steady-state temperature was reached. A large heating power can produce considerable thermal energy, which leads to a high steady-state.[12–17,26,33,38] On the other hand, the higher steady-state temperature was observed in a mild acid-treated sheet at a given input voltage [Fig. 3(c)]. Randomly disjoint individual MWCNTs were connected to provide continuous electrical pathways after the acid treatment, which results in a decrease in resistance.[34,36] The MWCNT sheets were made from numerous individual MWCNTs, of which some MWCNTs in the sheet might be separated and be unable to generate heat (Fig. 4). They should be interconnected with each other to allow the flow of carriers between the electrodes. The thickness of the MWCNT sheets decreased after the acid treatment, which means the effective density increased. The mild acid treatment of the MWCNT sheet ensured highly interconnected individual MWCNTs, which makes them electrically contiguous. In addition, high purity MWCNTs were obtained after the acid treatment due to the removal of amorphous carbon as seen in Fig. 5. Therefore, increasing the number of connected MWCNTs by immersing them in acid is the main reason for the improvement, along with the cleaning of their surfaces.[41] This is a highly favorable structural feature that achieves a higher thermal performance.

To further enhance the thermal characteristics, Ni nanoparticles were deposited on the sheet to increase the number of contact points between the MWCNTs. By Eq. (1), it is important to increase the surface area and number of contact points to improve the level of heat generation. In order to increase the surface area, the sheets are comprised of overlapped double layers on a substrate. Figure 3(b) shows that much higher steady-state temperature reaches at double layer sheet. A previous study reported that heat generation increases with increasing number of layers.[26,33] The surface of the MWCNT sheets had greater porosity, which means that the surface area and heating characteristics of the MWCNT sheet are strongly dependent on the changes in the film.

Metal nanoparticles are prepared by electrodeposition onto CNT sheets. This is a useful and easy way to increase the interconnections between CNTs for heat generation. As mentioned previously, the MWCNT sheet is formed by hundreds of thousands of individual CNTs.[42] As metal nanoparticles are added to the MWCNT sheet, it causes further interconnection of the individual CNTs. Moreover, the effective heat dissipation of the MWCNT sheet can be increased by adding metal nanoparticles because metal nanoparticles

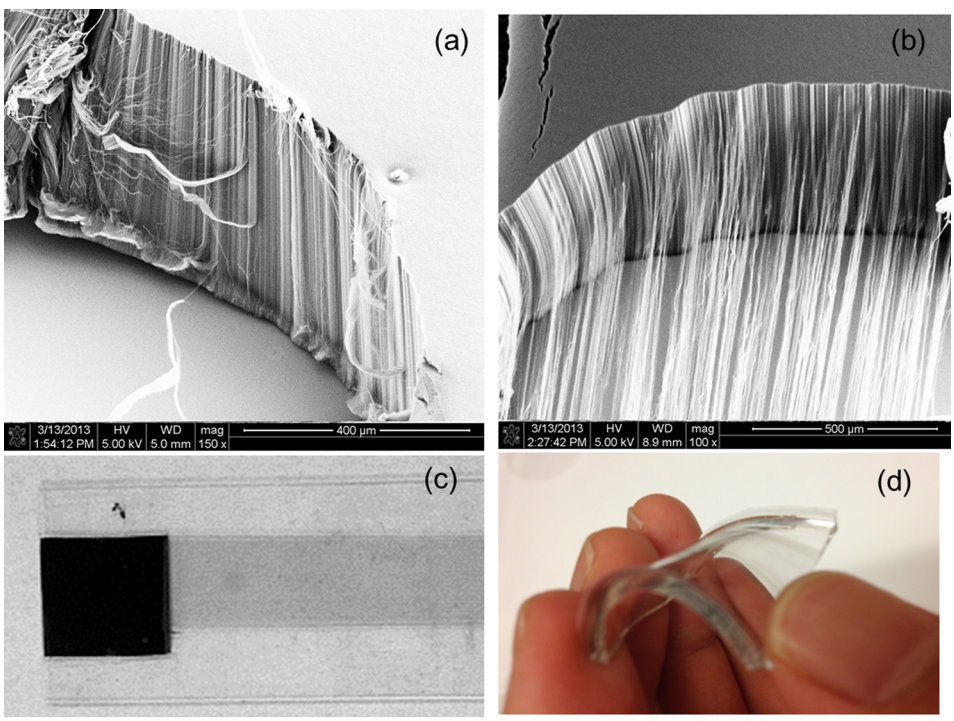

FIG. 2. (Color online) SEM images and a photograph of (a) spin-capable CNT forests with good alignment of 430 μm MWCNTs, (b) CNTs sheet pulling from the CNTs forest, sheet transfer from the Si substrate to (c) glass substrate and (d) PDMS substrate.

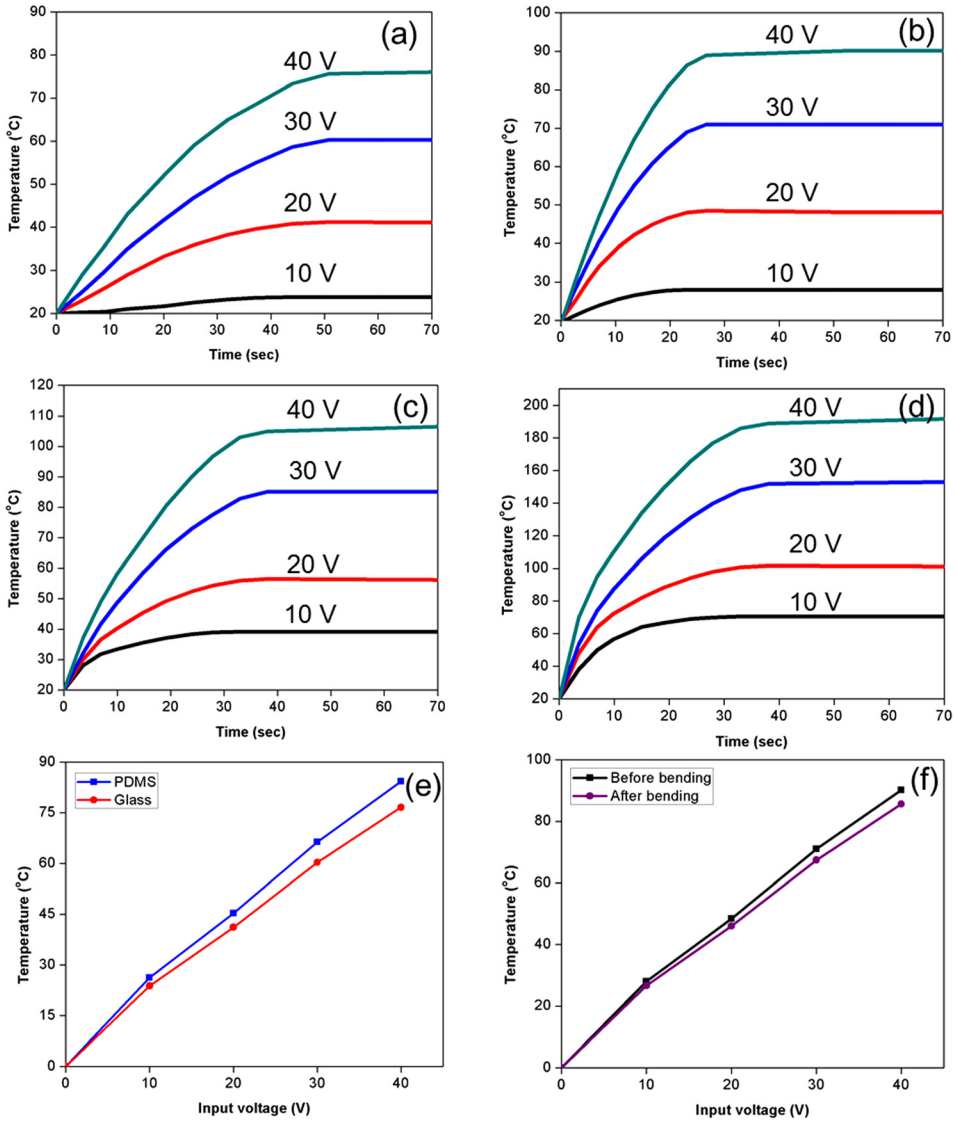

FIG. 3. (Color online) Electro-heating performance of MWCNT sheet films on glass; Time vs temperature profiles with respect to different applied voltages for (a) one layer, (b) double layers, (c) acid treated one layer, (d) decorated with Ni, (e) steady-state temperatures as a function of the input power on PDMS and glass substrates, and (f) temperature profiles after the bending tests.

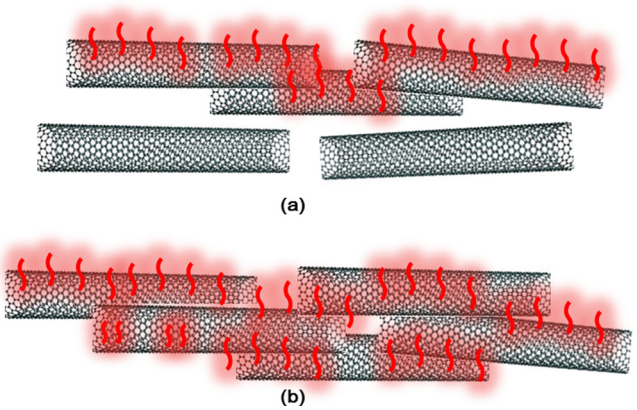

FIG. 4. (Color online) Schematic views of disconnected and connected CNTs in sheet (a) before and (b) after acid treatment, respectively.

can generate heat on their surface, which leads to an increase in the ability to generate heat in the CNTs sheet, as shown in Fig. 6. Figure 3(d) clearly shows that the CNT/Ni sheet has much better heating performance than the pure CNT and acid treated CNT sheet.

A major advantage of using a CNT sheet for the fabrication of TCF arises from the fact that high flexibility can be achieved, which is clearly not the case with ITO-based TCF. A flexible sheet was prepared on polydimethylsiloxane (PDMS) substrates. The experiments were carried out using a 1 mm thick PDMS substrate. As shown in Fig. 3(e), the steady state temperatures obtained on PDMS were slightly higher than those obtained on glass at the given applied voltages. Moreover, the heating rate was more than 1.7–2 °C/s higher at an applied voltage of 40 V. This means that less power is required to reach a given temperature on PDMS compared to the glass substrate. This might be due to the difference in thermal conductivity of the substrate materials [λ_{sub} in Eq. (7)]. Heat conducts more readily to the substrate when a

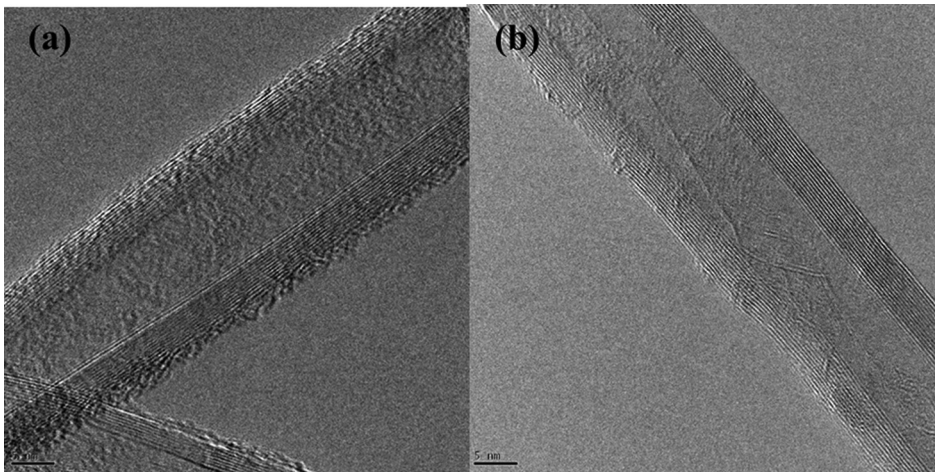

FIG. 5. TEM images of the CNTs in sheet (a) before and (b) after acid treatment, respectively.

material has a high thermal conductivity. The thermal conductivity of PDMS was ~0.18 W/m°C,[43,44] whereas glass has a significantly higher thermal conductivity (~1.05 W/m°C). This suggests that heat transfer is lower with the PDMS substrate. Therefore, the heating rate and steady state temperature are slightly higher compared to the glass substrate.

During the bending experiments (2.5 mm of bending radius), bending was performed hundreds of times to examine the mechanical durability and flexibility of the samples. After the bending cycles, no visible changes were observed in the morphology, and similar sheet resistances were maintained regardless of the bending constraints applied to the samples. These samples on the PDMS substrates were extremely flexible. As shown in Fig. 3(f), similar steady-state temperatures were observed before and after bending deformation (single MWCNT-sheet). This outstanding performance might be due to the firmness and flexibility of the CNT sheet with the substrate. Therefore, the excellent mechanical properties of the CNT sheet can be applied to produce a transparent flexible heater.

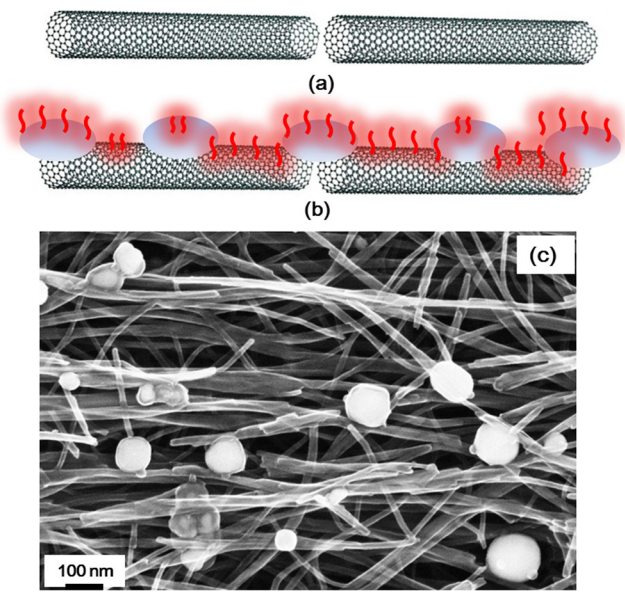

FIG. 6. (Color online) Schematic diagrams and SEM image of the disconnected CNTs in sheet; (a) before and (b) and (c) after Ni deposition.

IV. SUMMARY AND CONCLUSIONS

In summary, this paper presented a strategy for enhancing the heat performance of flexible transparent heaters using MWCNT sheets. The heating performance depends strongly on the surface area and the number of contact points between the individual CNTs (intertube contact). The surface area and contact point was increased in several ways: mild acid treatment, overlapped several sheet layers, and adding of metal nanoparticles. In particular, the heater was bent to examine the flexibility for flexible device applications. No obvious changes in resistance and morphology were observed after the bending test. Therefore, this method could be a useful approach for engineering highly flexible, transparent, and conducting films, which cannot be obtained using current TCF technology.

[1]S. Iijima, Nature **354**, 56 (1991).
[2]D. Jung. M. Han, L. J. Overzet, and G. S. Lee, J. Vac. Sci. Technol. B **31**, 06FI02 (2013).
[3]A. Nasiri, M. Shariaty-Niasar, A. M. Rashidi, and R. Khodafarin, Int. J. Heat. Mass. Transfer **55**, 1529 (2012).
[4]D. Jung. M. Han, and G. S. Lee, Sens. Actuators A **211**, 51 (2014).
[5]I. T. Clark, G. Rius, and Y. Matsuoka, J. Vac. Sci. Technol. B **28**, 1148 (2010).
[6]D. Jung. M. Han, and G. S. Lee, Mater. Lett. **122**, 281 (2014).
[7]D. Jung, K. H. Lee. D. Kim, L. J. Overzet, and G. S. Lee, J. Nanosci. Nanotechnol. **13**, 8275 (2013).
[8]D. Jung, J.-H. Kim, K. H. Lee, L. J. Overzet, and G. S. Lee, Diam. Relat. Mater. **38**, 87 (2013).
[9]D. Jung, M.-E. Han, and G. S. Lee, Mater. Lett. **116**, 57 (2014).
[10]S. L. Hellstrom *et al.*, Nano Lett. **12**, 3574 (2012).
[11]S. Zhang, C. Ji, Z. Bian, R. Liu, X. Xia, D. Yun, L. Zhang, C. Huang, and A. Cao, Nano Lett. **11**, 3383 (2011).
[12]K. Im, K. Cho, J. Kim, and S. Kim, Thin Solid film **518**, 3960 (2010).
[13]Z. P. Wu and J. N. Wang, Physica E **42**, 77 (2009).
[14]P. Xiao, J. W. Li, and R. Du, IEEE Trans. Nanotechnol. **10**, 520 (2011).
[15]X. Hou, K. L. Choy, and J. P. J. Liu, J. Nanosci. Nanotechnol. **11**, 8114 (2011).
[16]A. Stadler, Materials **5**, 661 (2012).

[17]Y. Song, C. M. Yang, D. Y. Kim, H. Kanoh, and K. J. Kaneko, Colloid Interface Sci. **318**, 365 (2008).
[18]J. Lewis, Mater. Today **9**, 38 (2006).
[19]Y. Letterier, L. Medico, F. Demarco, J. A. E. Manson, U. Betz, M. F. Escola, M. K. Olsson, and F. Atammy, Thin Solid Films **460**, 156 (2004).
[20]M. W. Rowell, M. A. Topinka, M. D. McGehee, H.-J. Prall, G. Dennler, N. S. Sariciftci, L. Hu, and G. Gruner, Appl. Phys. Lett. **88**, 233506 (2006).
[21]E. H. Lee, J. H. Ryu, J. Jang, and K. C. Park, Jpn. J. Appl. Phys. **50**, 03CA04 (2011).
[22]F. Bonaccorso, Z. Sun, T. Hasan, and A. C. Ferrari, Nat. Photonics **4**, 611 (2010).
[23]J. M. Kang, H. K. Kim, K. S. Kim, S. K. Lee, S. K. Bae, J. H. Ahn, Y. J. Kim, J. B. Choi, and B. H. Hong, Nano Lett. **11**, 5154 (2011).
[24]Y.-H. Yoon, J.-W. Song, D. Kim, J. Kim, J.-K. Park, S.-K. Oh, and C.-S. Han, Adv. Mater. **19**, 4284 (2007).
[25]D. Kim, H.-C. Lee, J. Y. Woo, and C.-S. Han, J. Phys. Chem. C **114**,5817 (2010).
[26]T. J. Kang, T. Kim, S. M. Seo, Y. J. Park, and Y. H. Kim, Carbon **49**, 1087 (2011).
[27]Y.-L. Li, L. A. Kinloch, and A. H. Windle, Science **304**, 276 (2004).
[28]M. Zhang, S. Fang, A. A. Zakhidov, S. B. Lee, A. E. Aliev, C. D. Williams, R. K. Atkinson, and R. H. Baughman, Science **309**, 1215 (2005).
[29]K. H. Lee, D. W. Jung, D. Burk, L. J. Overzet, and G. S. Lee, J. Vac. Sci. Technol. B **30**, 041809 (2012).
[30]D. Jung, K. H. Lee, L. J. Overzet, and G. S. Lee, IEEE Trans. Nanotechnol. **13**, 349 (2014).
[31]D. W. Jung, K. H. Lee, J. H. Kim, D. Burk, L. J. Overzet, G. S. Lee, and S. H. Kong, J. Nanosci. Nanotechnol. **12**, 5663 (2012).
[32]D. Jung, M. Han, and G. S. Lee, Appl. Phys. Express **7**, 025102 (2014).
[33]D. Jung, D. Kim, K. H. Lee, L. J. Overzet, and G. S. Lee, Sens. Actuators A **199**, 176 (2013).
[34]H.-S. Jang, S. K. Jeon, and S. H. Nahm, Carbon **49**, 111 (2011).
[35]H. Im, E. Y. Jang, A. Choi, W. J. Kim, T. J. Kang, Y. W. Park, and Y. H. Kim, Appl. Mater. Interfaces **4**, 2338 (2012).
[36]D. Jung, K. H. Lee, D. Kim, D. Burk, L. J. Overzet, and G. S. Lee, Jpn. J. Appl. Phys. **52**, 03BC03 (2013).
[37]See supplementary material at http://dx.doi.org/10.1116/1.4876127 for preparing samples and experimental procedures.
[38]J. J. Bae *et al*., Adv. Funct. Mater. **22**, 4819 (2012).
[39]J. Courbat, M. Canonica, D. Teyssieux, D. Briand, and N. F. D. Rooij, J. Micromech. Microeng. **21**, 015014 (2011).
[40]S. Mazumder and A. Majumdar, J. Heat Transfer **123**, 749 (2001).
[41]H. Z. Geng, K. K. Kim, K. P. So, Y. S. Lee, Y. Chang, and Y. H. Lee, J. Am. Chem. Soc. **129**, 7758 (2007).
[42]D. Jung, Y. Yoon, and G. S. Lee, Chem. Phys. Lett. **577**, 96 (2013).
[43]C. Chou and M.-H. Yang, J. Thermal Anal. **40**, 657 (1993).
[44]H.-S. Chuang and S. J. Wereley, J. Micromech. Microeng. **19**, 045010 (2009).